Accepted Manuscript

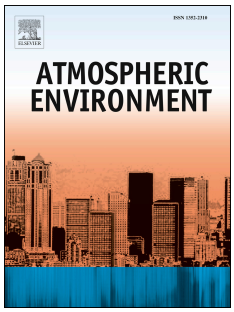

Quantification of manganese species in particulate matter collected in an urban area nearby a manganese alloy plant

A. Hernández-Pellón, P. Mazón, I. Fernández-Olmo

PII: S1352-2310(19)30138-4

DOI: https://doi.org/10.1016/j.atmosenv.2019.02.040

Reference: AEA 16582

To appear in: *Atmospheric Environment*

Received Date: 17 October 2018

Revised Date: 22 January 2019

Accepted Date: 24 February 2019

Please cite this article as: Hernández-Pellón, A., Mazón, P., Fernández-Olmo, I., Quantification of manganese species in particulate matter collected in an urban area nearby a manganese alloy plant, *Atmospheric Environment*, https://doi.org/10.1016/j.atmosenv.2019.02.040.

Quantification of manganese species in particulate matter collected in an urban area nearby a manganese alloy plant

A. Hernández-Pellón[a*], P. Mazón[a] and I. Fernández-Olmo[a]

[a] Dpto. de Ingenierías Química y Biomolecular, Universidad de Cantabria, Avda. Los Castros s/n, 39005 Santander, Cantabria, Spain

*Corresponding author
Dpto. de Ingenierías Química y Biomolecular, Universidad de Cantabria, Avda. Los Castros s/n, 39005 Santander, Cantabria, Spain
ana.hernandez@unican.es

Abstract

A sequential extraction test was used to evaluate the manganese (Mn) species in PM_{10} samples collected in an urban area impacted by a Mn alloy plant, where the annual guideline value for Mn in air according to the World Health Organization (WHO) is frequently exceeded (i.e. > 150 $ng \cdot m^{-3}$). The average Mn level in this campaign was 208.6 $ng \cdot m^{-3}$, reaching maximum daily values up to 1138.9 $ng \cdot m^{-3}$. Manganese species were dominated by water-soluble Mn (49.9%), followed by metallic Mn (Mn^0) and Mn^{2+} (27.1%), insoluble Mn (14.6%), and Mn^{3+} and Mn^{4+} (8.8%). This study reveals, on one hand, the higher fraction of water-soluble Mn species present in atmospheric aerosols in comparison with aerosols collected in work environments of the Mn alloy industry, which is attributed to the reaction between emitted Mn oxides and gaseous pollutants (SO_2, NO_2 and HCl) during transport in the atmosphere. On the other hand, there was a non-negligible fraction of more toxic species (Mn^{3+} and Mn^{4+}), which are more potent than Mn^{2+} to induce reactive oxygen species.

Keywords

Manganese; Speciation; PM_{10}; Manganese alloy plant; Environmental exposure

1. Introduction

Air manganese (Mn) overexposure is an important cause of concern in urban areas affected by the activity of the Mn alloy industry. Although Mn is vital for the human body, recent studies suggest that Mn chronic exposure is associated with neurotoxic disorders (Lucchini et al., 2012; Menezes-Filho et al., 2011). In this regard, despite the lack of a European regulation that establishes limit values for Mn in air, the World Health Organization (WHO) has proposed an annual average guideline value of 150 $ng \cdot m^{-3}$. This recommendation is frequently exceeded in areas affected by the emissions from Mn alloy plants (Hernández-Pellón and Fernández-Olmo, 2019).

Mn toxicity is associated with the size and morphology of the Mn-bearing particulate matter (PM), which determine the fate of this pollutant into the respiratory tract (Thomassen et al., 2001); in addition, the chemical speciation of Mn compounds and more specifically the Mn oxidation state strongly affects its toxicity (Majestic et al., 2007). The oxidation state is a key factor in relation with Mn ability to induce reactive oxygen species (ROS). Many of the adverse health effects caused by PM can be triggered by the oxidative stress caused by the ROS generation (Xiang et al., 2016). These species are also known due to their capacity to oxidize lipids and proteins or damage DNA, increasing the inflammatory response, which can lead to numerous diseases, mainly respiratory diseases (He et al., 2018; Peixoto et al., 2017; Van Den Heuvel et al., 2016; Xiang et al., 2016). In this regard, oxidized forms of Mn such as Mn^{3+} are more potent than Mn^{2+} to induce ROS (Ali et al., 1995). Studies dealing with the physico-chemical characterization of Mn-bearing particles associated with the emissions from Mn alloy plants have mainly focused on: (i) the evaluation of the size, morphology and chemical composition of the individual particles by using electron microscopy analysis (e.g. SEM-EDX and TEM-EDX analysis) (Arndt et al., 2016; Gjønnes et al., 2011; Gunst et al., 2000; Hernández-Pellón et al., 2017; Marris et al., 2012, 2013), (ii) the identification of the crystallographic phases by X-ray diffraction techniques (Hernández-Pellón et al., 2017; Marris et al., 2013), and (iii) the determination of the Mn solubility in simulated lung fluids (SLFs) as an estimation of its potential bioaccessibility into the human body (Hernández-Pellón et al., 2018; Mbengue et al., 2015). Only a few studies deal with the quantitative determination of the Mn species, all being related to Mn occupational exposure (Ellingsen et al., 2003;

Thomassen et al., 2001). To our knowledge, none of them aim to quantify the Mn species associated with ambient air Mn exposure.

In this study, a sequential extraction test was used to investigate the Mn species present in PM_{10} samples collected in an urban area located near a Mn alloy plant, where high Mn levels in air, according to the WHO criteria, have been previously reported (Hernández-Pellón and Fernández-Olmo, 2019; Moreno et al., 2011).

2. Materials and methods

The study was carried out in Maliaño, a town located in the southern part of the Santander Bay (Cantabria, northern Spain). A PM_{10} sampling campaign was conducted in May-June 2016 on the rooftop of "La Vidriera" cultural center (CCV site, UTM, 30T, X=431899, Y=4807290) located 350 m from a Mn alloy plant, which specializes in FeMn and SiMn alloy production. A total of 28 daily PM_{10} samples were collected on 47 mm quartz fiber filters (Sartorius) by a low volume sampler device (2.3 $m^{3}{\cdot}h^{-1}$) equipped with a 15-filter cartridge. Figure 1 shows the location of the CCV site and Mn alloy plant and the wind rose during the sampling period.

After a gravimetric determination, the filters were cut into three pieces. One quarter of the filter was used for the determination of the total Mn content, whereas the remaining filter was divided into two equal portions and subjected to a sequential extraction test (two replicates per filter). The total Mn content was determined based on the European standard method "EN-UNE 14902:2006", which consisted in an acid digestion of the filter in a microwave digestion system (Milestone Ethos One) using closed PTFE vessels (HNO_3:H_2O_2 with a mixture of 8:2 ml, up to 220 ºC). The Mn species were determined by a four-step sequential extraction test based on the methodology developed by Thomassen et al. (2001). Table 1 shows the optimized leaching conditions for the different Mn species. The sequential extraction procedure was carried out as follows:

Step 1: A portion of 3/8 of each filter (two replicates per filter) was introduced into a 50 ml polypropylene tube with a 25 ml filter cup insert equipped with 0.2 µm PVDF membrane obtained from ThermoScientific. A volume of 10 ml of ammonium acetate (0.01M) was added. The leaching test was then performed for 90 min with a rotatory shaker (10 rpm) (SBS). An incubator (MRHX-04, LSCI) was used to maintain the

temperature at 20ºC. After the leaching test was performed, the samples were centrifuged at 4200 rpm for 10 min.

The following steps of the sequential extraction test were carried out in the same microwave digestion system (Milestone Ethos One) and closed PTFE vessels used for the total Mn determination. After the leaching steps 2, 3 and 4, the content of the PTFE vessels was introduced in the mentioned polypropylene tubes equipped with 0.2 µm PVDF membranes and centrifuged at 4200 rpm for 10 min. Then the portion of filter was stored until further use.

Step 2: After being subjected to step 1, the portion of the filter was introduced in a closed PTFE vessel with 10 ml of acetic acid (25%). Then, the leaching test was carried out at 75ºC for 90 min.

Step 3: The extracting agent in this step consisted of 10 ml of a solution of hydroxylamine hydrochloride (5%) in acetic acid (25%). As in step 2, the leaching test was then performed at 75ºC for 90 min.

Step 4: The last step of the sequential extraction test consisted in an acid digestion (HNO_3:H_2O_2 with a mixture of 8:2 ml, up to 220 ºC) performed for 60 min.

The Mn concentrations in all the extracts were analyzed by inductively coupled plasma mass spectrometry (ICP-MS, Agilent 7500 CE). Quality control of the analytical procedure consisted in the determination of the recovery values from a standard reference material (NIST SRM 1648a, “Urban particulate matter”), as well as the evaluation of the blank contribution from the filters and reagents and subsequent subtraction from the results. In addition, yttrium was used as an internal standard to correct from instrumental drifts.

In addition, the comparison between the total Mn content determined by the digestion procedure and the sum of the Mn extracted in the four steps of the sequential extraction test was done to check the quality of the obtained results (r^2=0.98).

Statistical analysis of the data was performed using R statistical software version 3.0.0. All data distributions were checked for normality using the Shapiro-Wilks test. The interdependence between the total Mn content ($ng \cdot m^{-3}$), PM_{10} concentrations ($\mu g \cdot m^{-3}$) and the meteorological variables (temperature (ºC), precipitation (mm) and relative humidity (%)) was evaluated by determining the Pearson correlation coefficients.

3. Results and discussion

As Table 2 shows, despite the average PM_{10} concentration at the CCV site (26.6 $\mu g \cdot m^{-3}$) was well below the annual limit value established by Directive 2008/50/CE (40 $\mu g \cdot m^{-3}$), the mean air Mn concentration obtained in this campaign (208.6 $ng \cdot m^{-3}$) was above the 150 $ng \cdot m^{-3}$ recommended by the WHO as the annual guideline value, reaching maximum daily concentrations up to 1138.9 $ng \cdot m^{-3}$. As can be seen in Table 3, a strong correlation was found between the PM_{10} concentrations and the total Mn content present in the samples ($r=0.65$, $p<0.05$). In addition, the Mn values shown in this work are much lower in comparison with average Mn concentrations obtained in previous campaigns carried out at the CCV site in 2015 and 2017 (i.e. 721.9 $ng \cdot m^{-3}$ and 901.1 $ng \cdot m^{-3}$, respectively) (Hernández-Pellón et al., 2018; Hernández-Pellón and Fernández-Olmo, 2019). In this regard, mean values of temperature (20 ºC) and relative humidity (81.6 %) were similar to those usually found in spring in the same area. In addition, since the sampling campaign coincided with a period of low rainfall (average 1.3 mm/day), the lower Mn concentrations in air can not be explained due to the washing effect of precipitation in the atmosphere. In accordance with this, as Table 3 shows, no significant correlations were found between any of the mentioned variables and the total Mn content. However, the unusual wind pattern found during the sampling period could explain the measured Mn levels. Whereas most frequent winds in this region come from the S-SW direction, sending the plume emanating from the plant towards the CCV site, during this campaign, as Figure 1 shows, N was the predominant wind direction, which may lead to a lower influence of the Mn emissions from the Mn alloy plant on this sampling site.

Figure 2 presents the variability in the Mn speciation associated with the PM_{10} samples collected at the CCV site. The Mn species were dominated by water-soluble Mn (49.9%), followed by Mn^0 and Mn^{2+} (27.1%), insoluble Mn (14.6%), and Mn^{3+} and Mn^{4+} (8.8%).

In this regard, Marris et al. (2013) reported that particles collected in the near-field of a Mn alloy plant, analyzed by TEM combined with electron energy-loss spectroscopy (EELS), contained Mn with an oxidation state mainly between +II and + III. Also Ledoux et al. (2006) identified by electron paramagnetic resonance (EPR) different forms of Mn^{2+} species in areas affected by the emissions from a ferromanganese plant. Manganese dioxide (MnO_2), bixbyte (Mn_2O_3) and rhodochrosite ($MnCO_3$) were previously identified by XRD in PM_{10} samples collected in the studied area

(Hernández-Pellón et al., 2017). Additionally, Gjønnes et al. (2011) reported the presence of MnO and Mn_3O_4 associated with the FeMn alloy production from TEM observations.

Table 4 shows the comparison between the average percentages of the different Mn species obtained in this study and other works performed inside Mn alloy plants, with mixed FeMn/SiMn or only SiMn alloy production, using the same sequential extraction test (Ellingsen et al., 2003; Thomassen et al., 2001). Contrary to the results found in the present work, in which the water-soluble Mn compounds represented the highest percentage, Mn^0 and Mn^{2+} were the predominant species obtained in both respirable and inhalable aerosol samples collected in different areas inside mixed FeMn/SiMn alloy plants. The percentage of insoluble Mn in the work environments of these mixed FeMn/SiMn alloy plants was similar to the Mn insoluble fraction found in the PM_{10} in the present study. On the contrary, the presence of Mn^{3+} and Mn^{4+} in both respirable and inhalable aerosol samples was slightly higher in the other mixed FeMn/SiMn alloy production plants showed in Table 4 with respect to our study, obtaining similar values in plants dedicated only to SiMn alloy production, in both respirable and inhalable aerosols samples. Although Mn^0 and Mn^{2+} also presented a high contribution in the plants dedicated only to the production of SiMn alloys, in these plants the percentage of insoluble Mn species was also remarkable, this contribution being in some cases higher than the contribution of Mn^0 and Mn^{2+}, especially in the inhalable aerosol fraction (Ellingsen et al., 2003; Thomassen et al., 2001).

It should be noted that the comparison between the results presented in Table 4 should be done with caution due to the difference in the PM size fractions collected in each study. Both Thomassen et al. (2001) and Ellingsen et al. (2003) reported the quantification of the Mn species present in the inhalable and respirable aerosol fractions. The inhalable fraction is defined as the mass fraction of total airborne particles inhaled through the nose and mouth, whereas the respirable fraction is the mass fraction of inhaled particles penetrating to the unciliated airways (UNE-EN 481:1995). The particle sizes with 50% penetration for the inhalable and respirable fractions are 100 μm and 4.0 μm, respectively (UNE-EN 481:1995). In this regard, a previous characterization of PM_{10} samples collected at the CCV site showed that most of the Mn-bearing particles had mean diameters of less than 1 μm (Hernández-Pellón et al., 2017), and therefore they were included in the respirable fraction.

The greater presence of water-soluble Mn compounds in the PM_{10} samples collected at the CCV site with respect to the results reported in the different workroom environments inside Mn alloy plants (see Table 4) could be attributed to the changes of the particles emitted by this industrial activity during transport in the atmosphere. According to Marris et al. (2012) particles can evolve quickly in composition and size, forming agglomerates of metal-bearing particles and other supplementary mixed particles not existing inside the chimneys. In this regard, as Figure 1 shows, under the prevailing wind scenario during the sampling period (i.e. N direction) the plume emanating from the Mn alloy plant was not sent directly towards the CCV site, thus favoring the mixing of particles from different sources and allowing chemical transformations of the Mn compounds before reaching the sampling site.

No association was done in previous studies between the water-soluble Mn species extracted in the first step of the sequential extraction test and specific Mn compounds (Ellingsen et al., 2003; Thomassen et al., 2001). Since the water-soluble fraction was predominant in the PM_{10} samples collected at the CCV site, the knowledge about the oxidation states of these soluble compounds is of special interest in our study. In this regard, the presence of Mn in association with Cl or S was reported by Ledoux et al. (2006) in PM_{10} samples collected at a coastal area affected by the emissions from a ferromanganese plant. Also, Mn-bearing particles containing sulfates were detected in the plume emanating from a Mn alloy plant by Marris et al. (2012). Zhan et al. (2018) also suggested that PM-bound metals, such as Fe, Mn and Ni, can react with gaseous nitric acid in the atmosphere, leading to the formation of metal nitrates, which could increase the oxidative potential to a 200-600 %. As reported by Duvall et al. (2008) the increase in the water-soluble fraction of Mn in soil samples after reaction with gaseous nitric acid is especially evident. Thus, and based on the significant contribution of marine (Cl^-, Na^+ and SO_4^{2-}) and secondary inorganic aerosols ($SO_4^{2-}$and NO_3^{2-}) in the area of study (Orden MED/11/2012), the reactions between primary Mn-bearing particles and gaseous pollutants such as SO_2, NO_2 and HCl to form Mn soluble salts seem feasible. Two main hypotheses are established: (i) Mn soluble salts may result from the reaction of Mn oxides emitted by the Mn alloy plant with primary pollutants such as SO_2 and NO_2, as shown in reactions 1 and 2, or from the condensation of sulphuric or nitric acid on pre-existing particles (Marris et al., 2012) via reactions 3 and

4; (ii) highly soluble $MnCl_2$ could be form due to the reaction of Mn oxides with HCl depleted from aged sea salts via reactions 5-7.

$MnO_2 + SO_2 \rightarrow MnSO_4$ (1)

$MnO_2 + 2NO_2 \rightarrow Mn(NO_3)_2$ (2)

$MnO + H_2SO_4 \rightarrow MnSO_4 + H_2O$ (3)

$MnO + 2HNO_3 \rightarrow Mn(NO_3)_2 + H_2O$ (4)

$NaCl + HNO_3 \rightarrow NaNO_3 + HCl$ (5)

$2\ NaCl + H_2SO_4 \rightarrow Na_2SO_4 + 2\ HCl$ (6)

$MnO + 2HCl \rightarrow MnCl_2 + H_2O$ (7)

Assuming hypotheses (i) and (ii), the oxidation state of Mn in the species associated with the water-soluble fraction would be +II. Nevertheless, further work should be carried out to verify the oxidation state and chemical composition of the highly soluble Mn species found in this study. In the case that hypothesis (i) and (ii) were validated, and considering the first and partially the second step of the sequential extraction test, the predominant Mn oxidation state in the PM_{10} samples collected in the vicinity of the Mn alloy plant during the studied sampling period would be +II.

Regarding the implications on the ROS generation, the acid gas aging process of Mn^{2+} bearing particles from non-water soluble Mn oxides to water-soluble Mn species increases the oxidative potential of particulate matter, as suggested by Zhan et al. (2018), therefore, the potential changes in the oxidative potential of Mn-bearing particles due to chemical transformations during transport in the atmosphere should be further studied. In addition, in regard to the toxicity of these samples, the presence of a small fraction of Mn^{+3} and Mn^{+4} species (8.8 %) should not be neglected due to the greater capacity of these species to induce ROS with respect to Mn^{+2} (Ali et al., 1995).

From a health risk perspective, all the PM components that are soluble in different fluids should be considered. The evaluation of the bioaccessible fraction of metals (i.e. potentially available for absorption by the human body) is usually carried out by the study of their solubility in SLFs. In this regard, Figure 3 shows the comparison between the Mn soluble fractions (water-soluble and all soluble Mn species) derived from the sequential extraction test performed in this study and the Mn solubility reported in two common SLFs, Gamble's solution (pH=7.4) and artificial lysosomal fluid (ALF, pH=

4.5), in PM_{10} samples collected at the CCV site in a previous campaign (Hernández-Pellón et al., 2018). Gamble's solution is representative of the interstitial fluid in the deep lung, whereas ALF simulates the acidic intracellular conditions found in the lysosomes of alveolar macrophages (i.e. when the immune system of the body is reacting). As can be seen in Figure 3, although the samples were collected during different sampling periods, there is a good agreement between the sum of the Mn species obtained in the first three steps of the sequential extraction test (i.e. all soluble Mn compounds) and the Mn solubility in ALF at pH=4.5. However, the water-soluble Mn fraction found in this study (i.e. from samples collected under prevailing N winds) is higher with respect to the Mn solubility in Gamble's solution (pH=7.4) found in our previous work (i.e. with a predominant S-SW wind direction, sending the plume directly towards the sampling site) (Hernández-Pellón et al., 2018). In this regard, the joint study into the oxidation state and chemical composition, and the bioaccessibility of Mn species, taking into consideration the potential transformations of the emitted Mn species, is advisable to better assess the potential health risk of Mn environmental exposure near Mn alloy plants.

Conclusions

The manganese (Mn) species present in PM_{10} samples collected in an urban area nearby a Mn alloy plant were evaluated by a sequential extraction test. Manganese species followed the order: water-soluble Mn (49.9%), Mn^0 and Mn^{2+} (27.1%), insoluble Mn (14.6%), and Mn^{3+} and Mn^{4+} (8.8%). The percentage of water-soluble Mn species in the PM_{10} samples collected in this study was much higher in comparison with other results reported in work environments of the Mn industry. This difference was attributed to the formation of Mn soluble compounds due to the reaction of Mn oxides primary emitted by the Mn alloy plant with gaseous pollutants, such as SO_2, NO_2 and HCl.

Further work should be done to verify the oxidation state and chemical composition of the predominant highly soluble Mn species found in this study. In addition, a deeper understanding of the oxidation state, chemical composition and bioaccessibility of the Mn present in PM, as well as its potential changes during transport in the atmosphere, is vital to improve the assessment of the potential health risk of Mn environmental exposure nearby Mn alloy plants.

Acknowledgements

This work was financially supported by the Spanish Ministry of Economy and Competitiveness (MINECO) through the CTM2013-43904R Project. Ana Hernández-Pellón would like to thank the Ministry of Economy and Competitiveness (MINECO) for the FPI grant awarded, reference number BES-2014-068790.

References

Ali, S. F., Duhart, H. M., Newport, G. D., Lipe, G. W., Slikker Jr., W., 1995. Manganese-induced reactive oxygen species: Comparison between Mn^{+2} and Mn^{+3}. Neurodegeneration, 4(3), 329-334. doi:10.1016/1055-8330(95)90023-3

Arndt, J., Deboudt, K., Anderson, A., Blondel, A., Eliet, S., Flament, P., Fourmentin, M., Healy, R.M., Savary, V., Setyan, A., Wenger, J.C., 2016. Scanning electron microscopy-energy dispersive X-ray spectrometry (SEM-EDX) and aerosol time-of-flight mass spectrometry (ATOFMS) single particle analysis of metallurgy plant emissions. Environ. Pollut. 210, 9-17. doi:10.1016/ j.envpol.2015.11.019

Cantabria 2012, Orden MED/11/2012, de 28 de junio, por la que se aprueba el Plan de Mejora de la Calidad del Aire para partículas PM_{10} en el municipio de Camargo. Boletin oficial de Cantabria, 19 de junio de 2012, 140, 21606-21709

Duvall, R. M., Majestic, B. J., Shafer, M. M., Chuang, P. Y., Simoneit, B. R. T., Schauer, J. J., 2008. The water-soluble fraction of carbon, sulfur, and crustal elements in Asian aerosols and Asian soils. Atmos. Environ., 42(23), 5872-5884. doi:10.1016/j.atmosenv.2008.03.028

Ellingsen, D.G., Hetland, S.M., Thomassen, Y., 2003. Manganese air exposure assessment and biological monitoring in the manganese alloy production industry. J. Environ. Monit. 5, 84-90 doi:10.1039/b209095c

Gjønnes, K., Skogstad, A., Hetland, S., Ellingsen, D.G., Thomassen, Y., Weinbruch, S., 2011. Characterisation of workplace aerosols in the manganese alloy production industry by electron microscopy. Anal. Bioanal. Chem. 399, 1011-1020. doi:10.1007/s00216-010-4470-5

Gunst, S., Weinbruch, S., Wentzel, M., Ortner, H. M., Skogstad, A., Hetland, S., Thomassen, Y., 2000. Chemical composition of individual aerosol particles in workplace air during production of manganese alloys. J. Environ. Monit., 2(1), 65-71. doi:10.1039/a908329d

He, R.W., Shirmohammadi, F., Gerlofs-Nijland, M. E., Sioutas, C., Cassee, F. R., 2018. Pro-inflammatory responses to $PM_{0.25}$ from airport and urban traffic emissions. Sci. Total Environ., 640-641, 997-1003. doi:10.1016/j.scitotenv.2018.05.382

Hernandez-Pellón, A., Fernandez-Olmo, I., 2019. Using multi-site data to apportion PM-bound metal(loid)s: Impact of a manganese alloy plant in an urban area. Sci. Total. Environ. 651, 1476-1488. doi:10.1016/j.scitotenv.2018.09.261

Hernandez-Pellón, A., Fernandez-Olmo, I., Ledoux, F., Courcot, L., Courcot, D., 2017. Characterization of manganese-bearing particles in the vicinities of a manganese alloy plant. Chemosphere, 175, 411-424. doi:10.1016/j.chemosphere.2017.02.056

Hernández-Pellón, A., Nischkauer, W., Limbeck, A., Fernández-Olmo, I., 2018. Metal(loid) bioaccessibility and inhalation risk assessment: A comparison between an urban and an industrial area. Environ. Res., 165, 140-149. doi:10.1016/j.envres.2018.04.014

Ledoux, F., Laversin, H., Courcot, D., Courcot, L., Zhilinskaya, E.A., Puskaric, E., Aboukäis, A., 2006. Characterization of iron and manganese species in atmospheric aerosols from anthropogenic sources. Atmos. Res. 82, 622-632. doi:10.1016/j.atmosres.2006.02.018

Lucchini, R.G., Guazzetti, S., Zoni, S., Donna, F., Peter, S., Zacco, A., Salmistraro, M., Bontempi, E., Zimmerman, N.J., Smith, D.R., 2012. Tremor, olfactory and motor changes in Italian adolescents exposed to historical ferro-manganese emission. Neurotoxicology 33, 687-696. doi:10.1016/j.neuro.2012.01.005

Majestic, B.J., Schauer, J.J., Shafer, M.M., 2007. Development of a manganese speciation method for atmospheric aerosols in biologically and environmentally relevant fluids. Aerosol Sci. Technol. 41 (10), 925-933. doi:10.1080/02786820701564657

Marris, H., Deboudt, K., Augustin, P., Flament, P., Blond, F., Fiani, E., Fourmentin, M., Delbarre, H., 2012. Fast changes in chemical composition and size distribution of fine particles during the near-field transport of industrial plumes. Sci. Total Environ. 427-428, 126-138. doi:10.1016/j.scitotenv.2012.03.068

Marris, H., Deboudt, K., Flament, P., Grobety, B., Giere, R., 2013. Fe and Mn oxidation states by TEM-EELS in fine-particle emissions from a Fe-Mn alloy making plant. Environ. Sci. Technol. 47, 10832-10840. doi:10.1021/es400368s

Mbengue, S., Alleman, L. Y., Flament, P., 2015. Bioaccessibility of trace elements in fine and ultrafine atmospheric particles in an industrial environment. Environ. Geochem. Health, 37(5), 875-889. doi:10.1007/s10653-015-9756-2

Menezes-Filho, J. A., Novaes, C. de O., Moreira, J. C., Sarcinelli, P. N., Mergler, D., 2011. Elevated manganese and cognitive performance in school-aged children and their mothers. Environ. Res., 111(1), 156-163. doi:10.1016/j.envres.2010.09.006

Moreno, T., Pandolfi, M., Querol, X., Lavín, J., Alastuey, A., Viana, M., Gibbons, W., 2011. Manganese in the urban atmosphere: Identifying anomalous concentrations and sources. Environ. Sci. Pollut. Res., 18(2), 173-183. doi:10.1007/s11356-010-0353-8

Peixoto, M.S., de Oliveira Galvão, M.F., Batistuzzo de Medeiros, S.R., 2017. Cell death pathways of particulate matter toxicity. Chemosphere 188, 32–48. doi:10.1016/j.chemosphere.2017.08.076.

Thomassen, Y., Ellingsen, D. G., Hetland, S., Sand, G., 2001. Chemical speciation and sequential extraction of Mn in workroom aerosols: Analytical methodology and results

from a field study in Mn alloy plants. J. Environ. Monit., 3(6), 555-559. doi:10.1039/b104479f

Van Den Heuvel, R., Den Hond, E., Govarts, E., Colles, A., Koppen, G., Staelens, J., Mampaey, M., Janssen, N., Schoeters, G., 2016. Identification of PM10 characteristics involved in cellular responses in human bronchial epithelial cells (Beas-2B). Environ. Res. 149, 48–56. http://dx.doi.org/10.1016/j.envres.2016.04.029.

Xiang, P., He, R.W., Han, Y.H., Sun, H. J., Cui, X.Y., Ma, L. Q., 2016. Mechanisms of housedust-induced toxicity in primary human corneal epithelial cells: Oxidative stress, proinflammatory response and mitochondrial dysfunction. Environ. Int., 89-90, 30-37. doi:10.1016/j.envint.2016.01.008

Zhan, Y., Ginder-Vogel, M., Shafer, M.M., Rudich, Y., Pardo, M., Katra, I., Katoshevski, D., Schauer, J.J., 2018. Changes in oxidative potential of soil and fly ash after reaction with gaseous nitric acid. Atmos. Environ., 173, 306-315. doi:10.1016/j.atmosenv.2017.11.008

405 Table 1. Optimized leaching conditions for Mn species

Step	Oxidation state	Mn compounds	Reagent	Conditions
1	Water-soluble Mn	-	0.01 M ammonium acetate	90 min, 20ºC
2	Mn^0 and Mn^{2+}	Metallic Mn, FeMn, MnO, Mn_3O_4	25% acetic acid	90 min, 75ºC
3	Mn^{3+} and Mn^{4+}	Mn_2O_3, MnO_2, Mn_3O_4	0.5% hydroxylamine hydrochloride in 25% acetic acid	90 min, 75ºC
4	Insoluble Mn	SiMn	69% nitric acid-30% oxygen peroxide 8:2	60 min, 220ºC

406

407 Table 2. PM_{10} levels, total Mn content and meteorological conditions (precipitation,
408 temperature and relative humidity) at CCV during the sampling period. 28 daily values.

	PM_{10}	Total Mn	Precipitation	Temperature	Relative humidity
	$\mu g \cdot m^{-3}$	$ng \cdot m^{-3}$	mm/day	ºC	%
Mean	26.6	208.6	1.3	20	81.6
Median	27.1	83.2	0	20.4	82.1
SD	4.9	311.3	3.4	1.8	5.5
Min	16.3	5.8	0	16.5	70.6
Max	34.4	1138.9	17	24	90.9

409

410 Table 3. Pearson correlation coefficients between the total Mn content, PM_{10} levels and
411 meteorological variables. 28 daily samples.

	PM_{10}	P	T	HR
Total Mn	**0.65**	-0.11	0.17	0.01
PM_{10}		**-0.44**	0.23	0.15
P			**-0.48**	-0.12
T				0.32

412 P: Precipitation (mm); T: Temperature (ºC); HR: Relative humidity (%). In bold p value<0.05
413

414 Table 4. Comparison of the proportion of Mn species in % of the total Mn content in aerosol samples impacted by the Mn alloy industry

Production	Sample	Water-soluble Mn	Mn^0 and Mn^{2+}	Mn^{+3} and Mn^{+4}	Insoluble Mn	References
Mixed FeMn/SiMn alloys	PM_{10}	49.9	27.1	8.8	14.6	This study[a]
Mixed FeMn/SiMn alloys	Respirable	8-21*	57-62*	9-17*	13-18*	Thomassen et al. (2001)[b]
	Inhalable	8-21	50-54*	12-22*	16-24*	Thomassen et al. (2001)[c]
	Respirable	10.5	59.8	14.6	15.0	Ellingsen et al. (2003)[b]
	Inhalable	9.8	52.2	20.1	17.9	Ellingsen et al. (2003)[c]
Only SiMn alloys	Respirable	7-14	31-51*	7-10*	27-55*	Thomassen et al. (2001)[b]
	Inhalable	2-7	23-42*	6-11*	43-70*	Thomassen et al. (2001)[c]
	Respirable	11.2	47.2	9.3	32.3	Ellingsen et al. (2003)[b]
	Inhalable	5.0	37.9	9.0	48.1	Ellingsen et al. (2003)[c]

415

416 [a] PM_{10} samples collected 350 m from the Mn alloy plant
417 [b] Respirable aerosol samples collected in different areas inside the Mn alloy plants
418 [c] Inhalable aerosol samples collected in different areas inside the Mn alloy plants
419 * Minimum and maximum percentage
420
421
422

Figure captions

Figure 1. Location of the sampling site and manganese alloy plant. Wind rose of the sampling period (12 May-9 June 2016) developed with Openair tools. According to Beaufort scale, calm criteria 0.28 $m \cdot s^{-1}$.

Figure 2. Variability in the Mn species (%) associated with the PM_{10} samples collected at the CCV site, according to the sequential extraction test.

Figure 3. Comparison between the Mn soluble fractions (water-soluble and all soluble Mn species) derived from the sequential extraction test and the Mn solubility in two common SLFs (from Hernández-Pellón et al., 2018).

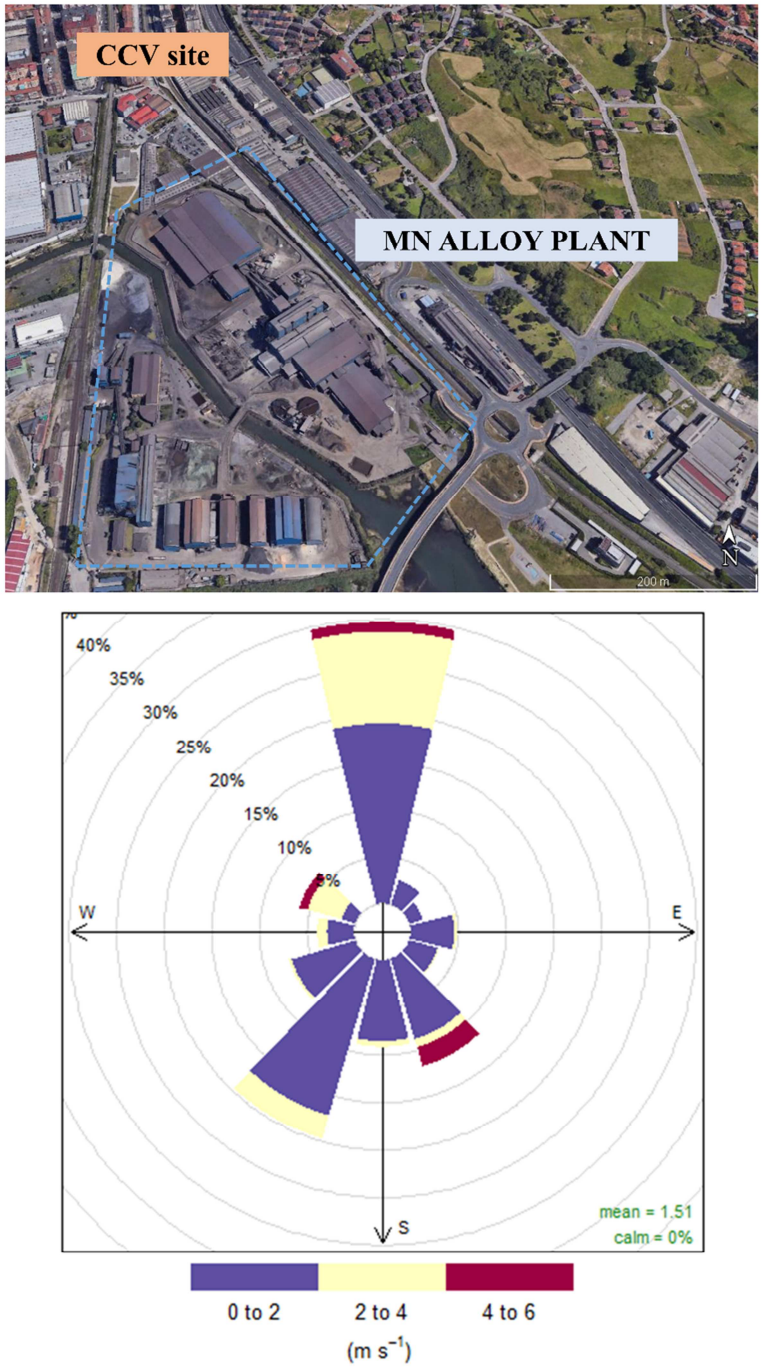

456
457

458 Figure 1. Location of the sampling site and manganese alloy plant. Wind rose of the
459 sampling period (12 May-9 June 2016) developed with Openair tools. According to
460 Beaufort scale, calm criteria 0.28 $m \cdot s^{-1}$.

461

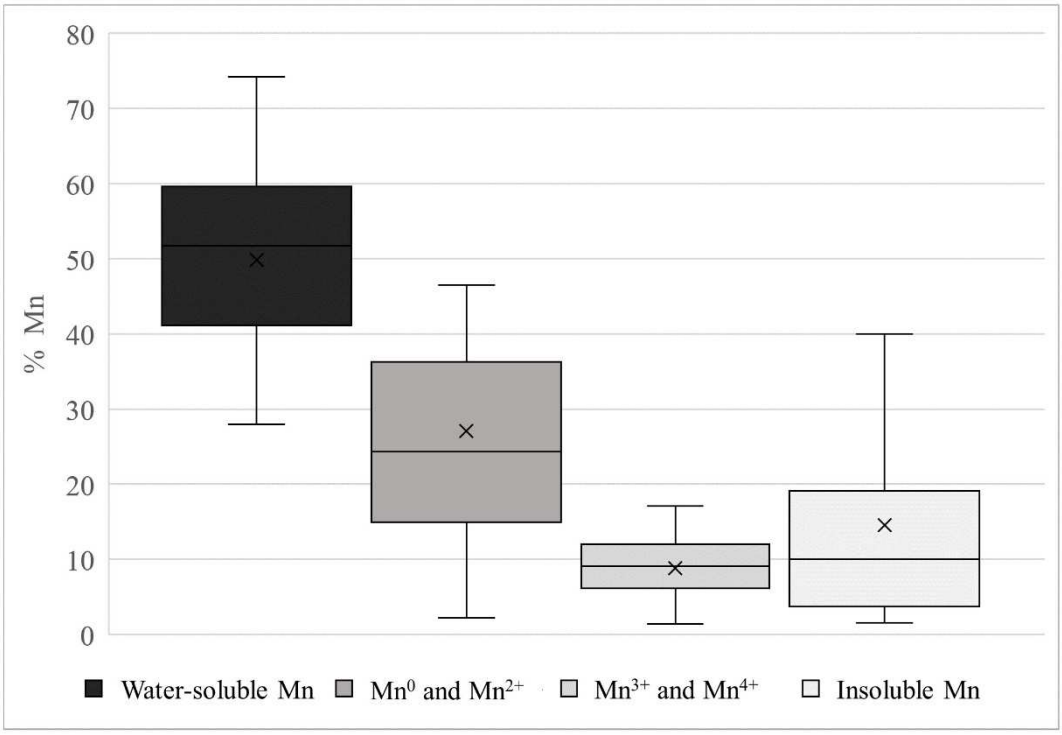

462

463

464 Figure 2. Variability in the Mn species (%) associated with the PM_{10} samples collected

465 at the CCV site, according to the sequential extraction test.

466

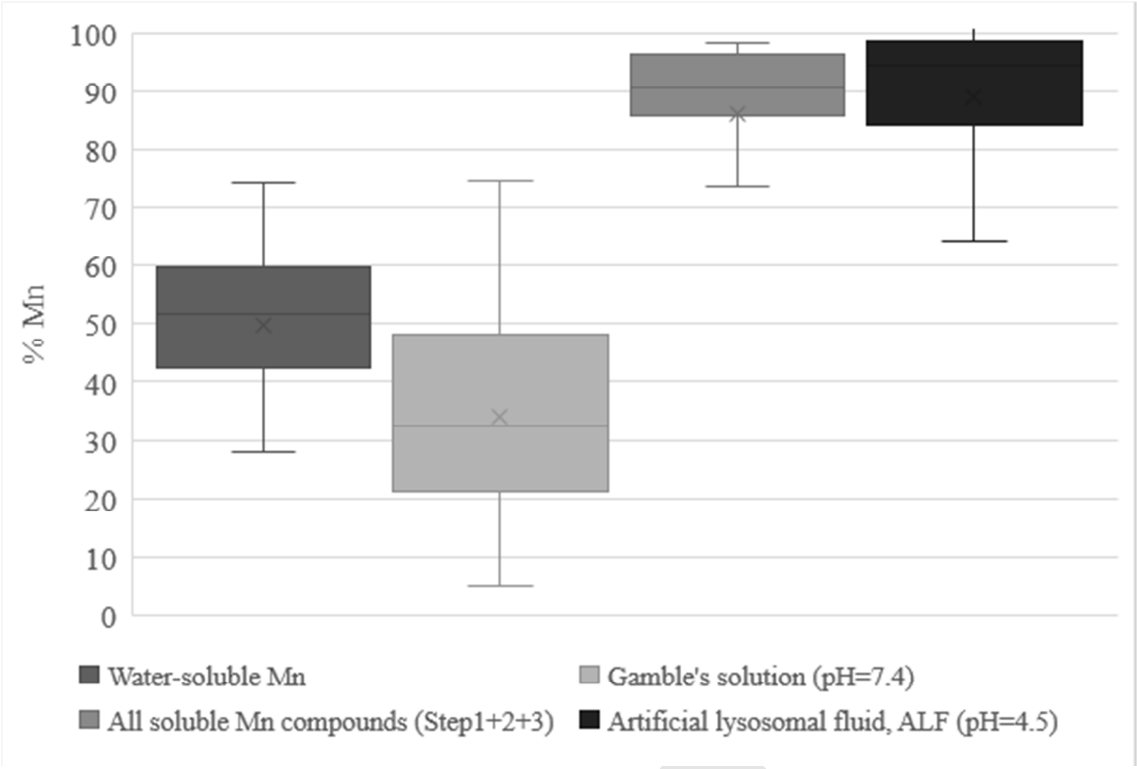

Figure 3. Comparison between the Mn soluble fractions (water-soluble and all soluble Mn species) derived from the sequential extraction test and the Mn solubility in two common SLFs (from Hernández-Pellón et al., 2018).

Table 1. Optimized leaching conditions for Mn species

Step	Components	Mn compounds	Reagent	Conditions
1	Water soluble Mn	-	0.01 M ammonium acetate	90 min, 20ºC
2	Mn^{0} and Mn^{2+}	Metallic Mn, FeMn, MnO, Mn_3O_4	25% acetic acid	90 min, 75ºC
3	Mn^{+3} and Mn^{4+}	Mn_2O_3, MnO_2, Mn_3O_4	0.5% hydroxylamine hydrochloride in 25% acetic acid	90 min, 75ºC
4	Insoluble Mn	SiMn	69% nitric acid-30% oxygen peroxide 8:2	60 min, 220ºC

Table 2. PM_{10} levels, total Mn content and meteorological conditions (precipitation, temperature and relative humidity) at CCV during the sampling period. 28 daily values.

	PM_{10}	Total Mn	Precipitation	Temperature	Relative humidity
	$\mu g \cdot m^{-3}$	$ng \cdot m^{-3}$	mm/day	ºC	%
Mean	26.6	208.6	1.3	20	81.6
Median	27.1	83.2	0	20.4	82.1
SD	4.9	311.3	3.4	1.8	5.5
Min	16.3	5.8	0	16.5	70.6
Max	34.4	1138.9	17	24	90.9

Table 3. Pearson correlation coefficients between the total Mn content, PM_{10} levels and meteorological variables. 28 daily samples.

	PM_{10}	P	T	HR
Total Mn	**0.65**	-0.11	0.17	0.01
PM_{10}		**-0.44**	0.23	0.15
P			**-0.48**	-0.12
T				0.32

P: Precipitation (mm); T: Temperature (ºC); HR: Relative humidity (%). In bold p value<0.05

Table 4. Comparison of the proportion of Mn species in % of the total Mn content in aerosol samples impacted by the Mn alloy industry

Production	Sample	Water-soluble Mn	Mn^0 and Mn^{2+}	Mn^{+3} and Mn^{+4}	Insoluble Mn	References
Mixed FeMn/SiMn alloys	PM_{10}	49.9	27.1	8.8	14.6	This study[a]
Mixed FeMn/SiMn alloys	Respirable	8-21[*]	57-62[*]	9-17[*]	13-18[*]	Thomassen et al. (2001)[b]
	Inhalable	8-21	50-54[*]	12-22[*]	16-24[*]	Thomassen et al. (2001)[c]
	Respirable	10.5	59.8	14.6	15.0	Ellingsen et al. (2003)[b]
	Inhalable	9.8	52.2	20.1	17.9	Ellingsen et al. (2003)[c]
Only SiMn alloys	Respirable	7-14	31-51[*]	7-10[*]	27-55[*]	Thomassen et al. (2001)[b]
	Inhalable	2-7	23-42[*]	6-11[*]	43-70[*]	Thomassen et al. (2001)[c]
	Respirable	11.2	47.2	9.3	32.3	Ellingsen et al. (2003)[b]
	Inhalable	5.0	37.9	9.0	48.1	Ellingsen et al. (2003)[c]

[a] PM_{10} samples collected 350 m from the Mn alloy plant
[b] Respirable aerosol samples collected in different areas inside the Mn alloy plants
[c] Inhalable aerosol samples collected in different areas inside the Mn alloy plants
[*] Minimum and maximum percentage